Gaucher disease mouse models: point mutations at the acid β-glucosidase locus combined with low-level prosaposin expression lead to disease variants

Ying Sun,* Brian Quinn,* David P. Witte,† and Gregory A. Grabowski[1],*

Division and Program in Human Genetics* and Division of Pediatric Pathology,† Children's Hospital Research Foundation, Cincinnati, OH 45229-3039

Abstract **Gaucher disease is a common lysosomal storage disease caused by a defect of acid β-glucosidase (GCase). The optimal in vitro hydrolase activity of GCase requires saposin C, an activator protein that derives from a precursor, prosaposin. To develop additional models of Gaucher disease and to test in vivo effects of saposin deficiencies, mice expressing low levels (4–45% of wild type) of prosaposin and saposins (PS-NA) were backcrossed into mice with specific point mutations (V394L/V394L or D409H/D409H) of GCase. The resultant mice were designated 4L/PS-NA and 9H/PS-NA, respectively. In contrast to PS-NA mice, the 4L/PS-NA and 9H/PS-NA mice displayed large numbers of engorged macrophages and nearly exclusive glucosylceramide (GC) accumulation in the liver, lung, spleen, thymus, and brain. Electron microscopy of the storage cells showed the characteristic tubular storage material of Gaucher cells. Compared with V394L/V394L mice, 4L/PS-NA mice that expressed 4–6% of wild-type prosaposin levels had ~25–75% decreases in GCase activity and protein in liver, spleen, and fibroblasts. These results imply that reduced saposin levels increased the instability of V394L or D409H GCases and that these additional decreases led to large accumulations of GC in all tissues. These models mimic a more severe Gaucher disease phenotype and could be useful for therapeutic intervention studies.**—Sun, Y., B. Quinn, D. P. Witte, and G. A. Grabowski. **Gaucher disease mouse models: point mutations at the acid β-glucosidase locus combined with low-level prosaposin expression lead to disease variants. *J. Lipid Res.* 2005.** 46: **2102–2113.**

Supplementary key words macrophage • lysosomal storage disease • glycosphingolipids

Gaucher disease is an autosomal recessive trait and the most common lysosomal storage disorder (1). The defective lysosomal hydrolysis of glucosylceramide (GC) in Gaucher disease is caused by mutations in the gene [human (GBA), mouse (*gba*)] encoding acid β-glucosidase (GCase), a membrane-associated lysosomal hydrolase (1). More than 200 mutations at the GBA locus have been identified in Gaucher disease patients, and the resultant defective or deficient enzyme activities lead to variable phenotypes (1, 2). The accumulation of GC leads to enlargement of the liver and spleen, bone lesions, and central nervous system (CNS) manifestations in some variants (1, 3–5). The macrophage is the primary cell displaying GC accumulation; nonmacrophage parenchymal cells appear normal in liver, lung, bone marrow, and spleen in Gaucher disease (e.g., hepatocytes, granulocytes, and lymphocytes) (1). The knock out of *gba* in the mouse leads to lethality in the newborn period (6). Efforts to create animal models of Gaucher disease with a longer life span have included the *gba* "knock in" of the L444P mutation, but this also led to early death attributable, at least in part, to a defective skin permeability barrier (7).

Additional mouse models were designed based on genotype/phenotype correlations in humans (8), as summarized in **Table 1**. Homozygosity for N370S in humans results in less severe to asymptomatic phenotypes (1, 9, 10). In comparison, homozygosity for the D409H allele is associated with early-onset, variable disease of the viscera and CNS (11, 12). These patients also can develop characteristic calcific abnormalities of the aortic valves and ascending aorta (13). The V394L allele has been observed only in the heteroallelic state, and when the heteroallele is L444P, the phenotype includes visceral and CNS involvement (11). In contrast, N370S homozygosity in mice was lethal in the neonatal period, V394L homozygosity displayed minor phenotypic abnormalities up to 12 months, and D409H or D409V homozygotes displayed low-grade Gaucher cell formation and GC storage (8). Visceral tis-

Manuscript received 19 May 2005 and in revised form 15 July 2005.

Published, JLR Papers in Press, August 1, 2005.
DOI 10.1194/jlr.M500202-JLR200

Abbreviations: CNS, central nervous system; *gba*, gene encoding mouse acid β-glucosidase; GC, glucosylceramide; GCase, acid β-glucosidase; LacCer, lactosylceramide; 4MU-Glc, 4-methylumbelliferyl-β-D-glucopyranoside; WT, wild-type.

[1] To whom correspondence should be addressed.
e-mail: greg.grabowski@cchmc.org

TABLE 1. Characteristics of humans and mice with GCase mutations

Genotype	Human	Mouse	References
D409H/D409H	Major visceral and CNS disease	Minor visceral disease	1, 8, 11, 12
D409V/L444P[a]	Major visceral and CNS disease	Minor visceral disease	1, 8
D409V/null		Major visceral disease	1, 8
N370S/N370S	Variable visceral disease	Death in neonatal period	1, 8, 9, 10
L444P/L444P	Variable visceral and CNS phenotypes	Death in neonatal period	1, 7
V394L/L444P or null[a]	Severe visceral and CNS disease	Minor visceral disease	1, 8
V394L/V394L[a]		Minor visceral disease	8

CNS, central nervous system; GCase, acid β-glucosidase.
[a] Homozygotes of D409V and V394L or V394L/null have not been observed in humans.

sues from homozygous murine models of V394L and D409H showed ⩽10% of wild-type (WT) GCase activity. Neither model displayed CNS involvement (8).

Saposins (sphingolipid activator proteins) A, B, C, and D are lysosomal glycoproteins that are encoded by a single gene, termed prosaposin (14–17). The saposins are essential to the optimal activity of glycosphingolipid hydrolases (18–21). In particular, saposin C is needed for full GCase function (22–24). Saposin C has at least two effects on GCase: *1*) optimization of GCase hydrolysis of GC and other substrates; and *2*) a protective effect for GCase against proteolytic digestion (24). This latter finding probably accounts for the reduction of GCase activity and protein levels in prosaposin-deficient mice and humans (24). In humans, deficiency of saposin C leads to a variant form of Gaucher disease with GC accumulation in macrophages and CNS (25). The proteolytic processing of prosaposin to the individual saposins occurs predominantly in acidified compartments, including the lysosome (26, 27). Prosaposin has been found in a variety of body fluids (14, 28).

To establish additional viable Gaucher disease mouse models and evaluate the in vivo effect of saposin C on mutant GCases, mice were created by cross-breeding V394L or D409H homozygotes into the PS-NA line that expresses subnormal levels of a transgene encoding mouse prosaposin/saposins. The resulting mice developed large accumulations of GC in a variety of tissues as a more florid viable analog of human Gaucher disease with CNS involvement.

MATERIALS AND METHODS

Materials

The following were from commercial sources: 4-methylumbelliferyl-β-D-glucopyranoside (4MU-Glc; Biosynth AG); sodium taurocholate (Calbiochem, La Jolla, CA); mouse anti-β-actin monoclonal antibody, trypsin, trypsin inhibitor, and primulin (Sigma, St. Louis, MO); NuPAGE 4–12% Bis-Tris gel, NuPAGE MES SDS running buffer, William's solution, collagenase, Ca/Mg-free HBSS, DMEM, neurobasal medium, and B27 supplement (Invitrogen, Carlsbad, CA); rat anti-mouse CD68 monoclonal antibody (Serotec, Oxford, UK); M-PER Mammalian Protein Extraction Reagent and BCA Protein Assay Reagent (Pierce, Rockford, IL); [^{35}S]cysteine/methionine protein labeling mix (DuPont-New England Nuclear Research Products, Boston, MA); Molecular Dynamics Storm 860 scanner, Hybond™-ECL™ nitrocellulose membrane, and ECL detection reagent (Amersham Biosciences, Piscataway, NJ); ABC Vectastain and Alkaline Phosphatase Kit II (black) (Vector Laboratory, Burlingame, CA); and BD TALON™ Metal Affinity Resin (BD Biosciences Clontech, Palo Alto, CA).

Mouse models

The mouse prosaposin cDNA was cloned from a λZap mouse liver library (29). It does not contain exon 8, which encodes amino acid QDQ in a saposin B region that appears nonessential (30). The mouse prosaposin transgene was created by cloning mouse prosaposin cDNA (2.5 kb) downstream from the 3-phosphoglycerate kinase promoter in the pBluescript vector. The prosaposin knockout ($PS^{-/-}$) mice containing this prosaposin transgene were generated previously and named PS-NA (31). The V394L and D409H point mutations at the mouse GCase locus were introduced using the cre-lox-P system (8). The crossing of V394L or D409H homozygotes with PS-NA resulted in 4L/PS-NA or 9H/PS-NA mice, respectively, with a genetic background of ∼50% FVB, 25% C57BL/6, and 25% 129SvEvBrd. D409V/D409V PS-NA mice were never observed from the appropriate crosses.

PCR genotyping

After mutation validation of GCase by direct sequencing, the lox-P site was used as a marker for GCase point mutation genotyping. Multiplex PCR was performed to genotype the point mutations and prosaposin transgene. For GCase point mutation, primers mGC4996F (5′-CACAGATGTGTATGGCCATCGG-3′ in intron 8 of GBA) and mGC5387R (5′-CTGAAGTGGCCAAGATGGTAG-3′ in exon 9 of GBA) generated a 391 bp fragment from WT and a 485 bp fragment (391 bp + 94 bp lox-P junction sequence in intron 8) for the mutant alleles (8). For the prosaposin transgene, primers CBC (5′-ATGAAGCTGGTGTCTGATGT-3′ in the saposin B region of the transgene) and PO8 (5′-CACAAATCCAGGATCCATCAC-3′ in the saposin D region of the transgene) yielded a 1 kb band. Reaction conditions were PCR buffer (Invitrogen) with 3 mM $MgCl_2$. Reactions were cycled 30 times as follows: 94°C for 60 s, 58°C for 60 s, and 72°C for 90 s. The prosaposin knockout allele was genotyped as described (31).

Histological studies

Mice were euthanized in age-matched groups. Liver, lung, spleen, thymus, brain, and spinal cord were collected, fixed in 10% formalin, embedded in paraffin, sectioned, and stained with hematoxylin and eosin and periodic acid-Schiff, then analyzed by light microscopy. Karnovsky's fixative was used for ultrastructural studies. For immunohistochemistry, frozen tissue sections fixed with 4% paraformaldehyde were incubated with rat anti-mouse CD68 monoclonal antibody (1:200 in PBS with 5% BSA) overnight at 4°C. Detection was performed using ABC Vectastain and Alkaline Phosphatase Kit II (black) according to the manufacturer's instruction. The slides were counterstained with methylene green.

Tissue lipid analyses

Tissue samples (~100 mg wet weight) in water (0.6 ml) and methanol (2 ml) were homogenized (PowerGen 35; Fisher Scientific), then chloroform (1 ml) was added. Homogenates were shaken (15 min) and centrifuged (5 min at 1,000 *g*). Pellets were reextracted with water (0.7 ml) and chloroform-methanol (1:2, v/v; 3 ml). The combined extracts were centrifuged (10 min at 7,000 *g*). The supernatants were transferred to fresh tubes and the solvents evaporated under N_2. Dried extracts were redissolved in chloroform-methanol-water (60:30:4.5, v/v/v; 15 ml) and desalted on Sephadex G-25 columns (32). Samples were then subjected to alkaline methanolysis (33) and desalted. Relative proportions of lipids from these tissue samples were determined by thin-layer chromatography with borate-impregnated plates (10 cm^2 Merck HPTLC silica gel 60; 200 μm) (34). Plates were developed in chloroform-methanol-water (65:25:4, v/v/v). Lipids were visualized with primulin spray (100 mg/l in 80% acetone) and blue fluorescence scanning (Storm 860; Amersham Pharmacia Biotech).

Enzyme activity assay

Tissues were homogenized in 1% sodium taurocholate and 1% Triton X-100, with 0.25% each in final assay mixtures. GCase activities were determined fluorometrically with 4MU-Glc (35). Some assay mixtures were preincubated in the presence and absence of the GCase irreversible inhibitor, conduritol B epoxide (1 mM, 40 min at 37°C). The substrate (4MU-Glc) was added, and the reactions were stopped after an additional incubation (30 min at 37°C) (36). WT activities of control tissues were determined in parallel for all assays. WT levels were set as 100%.

Preparation of anti-mouse prosaposin antiserum

The coding region of mouse prosaposin cDNA was cloned into pET21a vector and overexpressed in *Escherichia coli* as described (37). The expressed mouse prosaposin contained a 6 His tag at the carboxyl terminus. Harvested cell pellets were dissolved in 8 M urea (pH 8.0). The lysates were clarified by centrifugation (10,000 *g*, 25 min). The supernatants were mixed with BD TALON™ Metal Affinity Resin (cobalt-based) and gently agitated for 20 min to allow the His tag prosaposin binding to resin. The resin was washed with 25 mM imidazole, and the prosaposin protein was eluted with 150 mM imidazole, dialyzed, and analyzed by 10% SDS-PAGE. The single band products were used to raise goat antiserum (Harlan Bioproducts for Science, Madison, WI) after a 90 day protocol with initial inoculation of antigen (1 mg) and three boosts (500 μg each). Rabbit anti-mouse saposin D was raised against recombinant mouse saposin D produced in *E. coli* using the pET21a system (37). Using immunoblot analyses, goat anti-mouse prosaposin antiserum detected mouse prosaposin and saposins A, B, C, and D. Rabbit anti-mouse saposin D antiserum detected mouse saposin D and prosaposin.

Cell culture and immunoprecipitation

Hippocampal neurons were isolated from 17.5 day mouse embryos. The dissected hippocampi were digested with trypsin solution (1 mg/ml in HBSS, 20 min) at room temperature, and the tissues were transferred into trypsin inhibitor solution (1 mg/ml in HBSS) for 5 min, followed by washing in 2 ml of ice-cold HBSS. The tissues were dissociated, and the cells were plated in DMEM with 10% fetal bovine serum plus penicillin and streptomycin in polyethyleneimine-coated flasks. After 3 h, the medium was replaced with neurobasal medium with B27 supplement. The hippocampal neurons were allowed to grow for 5 days and then subjected to labeling and immunoprecipitation.

Hepatocytes were isolated from liver after perfusion with collagenase solution (0.2 mg/ml collagenase and 0.33 mM $CaCl_2$ in HBSS). Liver tissues were minced into small pieces with scissors and suspended in William's solution. The liver suspension was washed twice with William's solution, layered over the Percoll, and centrifuged (2 min at 800 *g*). The resultant pellets were washed twice in William's solution, and hepatocytes were plated in DMEM with 10% fetal bovine serum and 1% glutamine as well as penicillin and streptomycin in a 10 cm dish. The fresh medium was replaced after 1 h. The hepatocytes were allowed to grow for 7 days and then subjected to labeling and immunoprecipitation.

Mouse lung or tail fibroblasts were cultured in DMEM supplemented with 10% heat-activated fetal bovine serum as described previously (38). The above cells ($5–10 \times 10^5$ cells per flask) were labeled for 4 h with 127 μCi of [^{35}S]cysteine/methionine protein labeling mix. The media were collected and treated with anti-mouse saposin D antibody to precipitate the prosaposin protein. The proteins were resolved by SDS-PAGE as described (31).

Immunoblot

Tissues were homogenized in M-PER Mammalian Protein Extraction Reagent. Protein concentrations were estimated using BCA Protein Assay Reagent. Tissue extracts were separated on NuPAGE 4–12% Bis-Tris gels with NuPAGE MES SDS running buffer and electroblotted on Hybond™-ECL™ nitrocellulose membranes. The membranes were blocked with 5% nonfat dry milk for 1 h, followed by incubation overnight with goat anti-mouse prosaposin serum (1:500) diluted in 1% milk. The signal was developed using ECL detection reagent according to the manufacturer's instructions. The rabbit anti-mouse GCase IgG (1:1,500 in 0.15% milk and 0.1% BSA) was used to detect mouse GCase, and mouse anti-β-actin monoclonal antibody (1:10,000 in 2% milk) was applied to detect β-actin.

RESULTS

Creation of mouse models

To investigate the effect of saposins on GCase in vivo, the mouse models were generated by cross-breeding GCase point mutant (V394L or D409H) mice with prosaposin knockout ($PS^{-/-}$) mice or a hypomorphic prosaposin mouse line [i.e., $PS^{-/-}$ with a low-expressing mouse prosaposin transgene (PS-NA)] (**Table 2**). Both GCase mutant (V394L or D409H) mice were fertile and lived up to 2 years (8). The respective resultant cross-bred mice were designated 4L/PS-NA and 9H/PS-NA; these mice were fertile and survived up to 22 weeks. The PS-NA mice were fertile, with life spans up to 32 weeks (31). The $PS^{-/-}$ mice (i.e., prosaposin-null) generally die within 4 weeks (31, 39). The $4L/PS^{-/-}$ mice survived for 3–4 weeks, and they were infertile. Only limited numbers of $4L/PS^{-/-}$ and 9H/PS-NA mice were obtained; thus, only limited analyses were performed.

Prosaposin transgene expression

Transgenic saposin proteins in PS-NA mice were analyzed by immunoblots and scored relative to the levels of saposins in WT mice using goat anti-mouse prosaposin antiserum. This antibody reacts with prosaposin and all four saposins (A, B, C, and D). To correct for variations in the application amounts, the saposin levels were normalized to β-actin level on each gel. The amounts of transgenic sa-

TABLE 2. Characterization of mouse models

Genotype	Strains (%)	Life Span	Visceral Involvement	CNS Involvement	GCase[a]	Saposin	References
					% WT		
4L/PS-NA	FVB (50), C57BL/6 (25), 129SvEvBrd (25)	22 weeks	GC accumulation, engorged macrophages	GC accumulation, ataxia, waddling gait	3	6	Current
9H/PS-NA	FVB (50), C57BL/6 (25), 129SvEvBrd (25)	22 weeks	GC accumulation, engorged macrophages	GC accumulation, ataxia, waddling gait	nd	6	Current
4L/PS$^{-/-}$	FVB (50), C57BL/6 (25), 129SvEvBrd (25)	~4 weeks	GC accumulation, engorged macrophages	GC accumulation, ataxia, tonic status, epilepticus	nd	0	Current
PS-NA	FVB	32 weeks	Minor GC accumulation, occasional storage cells	Minor GC accumulation, ataxia, waddling gait	60	6	31, 24
PS$^{-/-}$	FVB	~4 weeks	Slight GC accumulation, occasional storage cells	Slight GC accumulation, ataxia, tonic status, epilepticus	25	0	31, 39, 24
V394L/V394L	C57BL/6 (50), 129SvEvBrd (50)	~2 years	Minor GC accumulation, occasional storage cells	No GC accumulation, normal phenotype	7	100	8
D409H/D409H	C57BL/6 (50), 129SvEvBrd (50)	~2 years	Minor GC accumulation, occasional storage cells	No GC accumulation, normal phenotype	~4	100	8

4L/PS-NA = V394L/V394L + PS$^{-/-}$ + low-level mouse prosaposin transgene expression; 4L/PS$^{-/-}$ = V394L/V394L + PS$^{-/-}$; 9H/PS-NA = same as 4L/PS-NA, except with D409H/D409H; PS-NA = PS$^{-/-}$ with low-level mouse prosaposin transgene expression; PS$^{-/-}$ = prosaposin null. GC, glucosylceramide; WT, wild-type.

[a] GCase activity and saposin protein levels in liver; nd, not done.

posin protein levels varied with the tissue source and were 4–45% of WT levels (**Fig. 1A**). These levels were consistent in the specific tissue and did not vary significantly within or among the various mouse strains.

After metabolic labeling, the secretion of transgenic prosaposin was assessed by immunoprecipitations of cell culture media using rabbit anti-mouse saposin D antibody. Transgenic prosaposin was detected in medium from cultured fibroblasts, hippocampal neurons, and hepatocytes of PS-NA mice (Fig. 1B). The transgenic prosaposin was

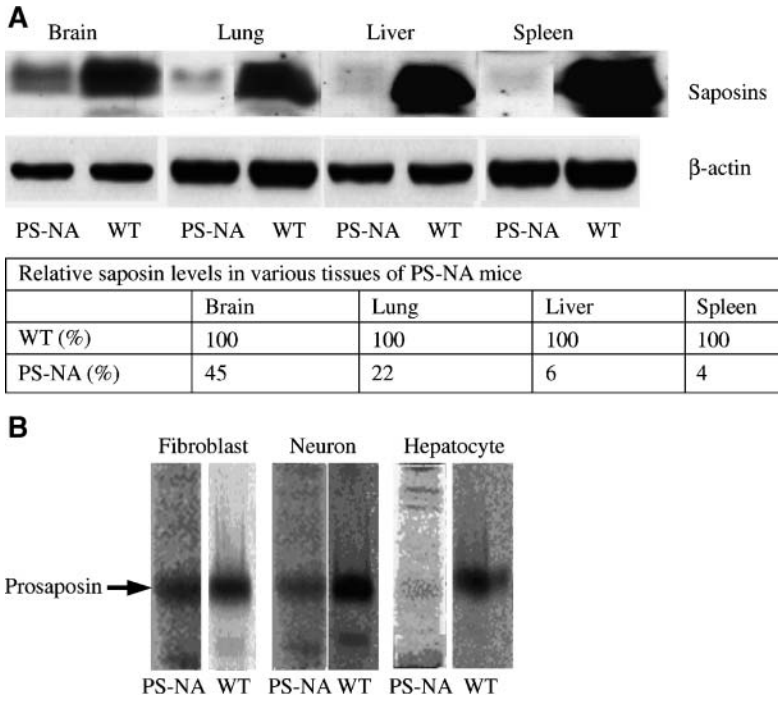

Relative saposin levels in various tissues of PS-NA mice				
	Brain	Lung	Liver	Spleen
WT (%)	100	100	100	100
PS-NA (%)	45	22	6	4

Fig. 1. Prosaposin levels and secretion in PS-NA mouse tissues. A: Transgenic saposin protein levels in PS-NA mouse tissues were resolved by SDS-PAGE in brain (100 μg of protein) and liver, lung, and spleen (250 μg of protein). The saposins (M_r ~ 10,000) were detected using goat anti-mouse prosaposin antibody that detects saposins A, B, C, and D as well as prosaposin. Quantification of saposin levels in PS-NA mice for each tissue is presented as a percentage of wild-type (WT) levels after normalization to a β-actin loading control. Each experiment was repeated three times with the lysates from different mice. Quantitation was performed using Molecular Dynamics ImageQuant Software. B: Secretion of transgenic prosaposin. Proteins from primary cells (fibroblast, hippocampal neuron, and hepatocyte) from PS-NA and WT mice were labeled with [^{35}S]cysteine/methionine for 4 h. Prosaposin (arrow) in equal volumes of cell medium was immunoprecipitated with rabbit anti-mouse saposin D antibody.

secreted at a lower level than in comparable samples from WT mice. This was evaluated because exon 8, which encodes the amino acids QDQ in the prosaposin gene, has been proposed to be a secretion signal (14, 40) and the prosaposin transgene in PS-NA mice does not contain exon 8. Thus, these results demonstrate that the prosaposin transgene produces a prosaposin protein that is processed into saposins and is also secreted intact in relative proportion to its expression levels in whole tissue extracts (compare Fig. 1A, B).

Visceral tissues

By light microscopy, the visceral organs of PS-NA mice had rare scattered storage cells in liver, spleen, and thymus only near the end stage (~32 weeks). Similarly, the V394L/V394L and D409H/D409H mice displayed only a few scattered storage cells in these tissues at very late stages (>18 months). In comparison, 4L/PS-NA and 9H/PS-NA mice displayed large numbers of storage cells in liver, lung, spleen (**Fig. 2**), and thymus. Clusters of such cells were easily visible in these mice at 4 weeks. The numbers and sizes of the storage cells increased with age. Overall, the numbers and clusters of storage cells were greatest in the 4L/PS-NA mice. Electron microscopy of such storage cells of 4L/PS-NA mice showed the characteristic braided structure of stored GC (**Fig. 3**), similar to those observed in human Gaucher cells (1, 5, 41). Additionally, residual bodies containing remnants and undigested material were seen on ultrastructure of such cells from liver and spleen of 4L/PS-NA mice (data not shown). The nature of the storage cells in 4L/PS-NA and 9H/PS-NA mouse tissues was evaluated by immunohistochemistry using anti-CD68 antibody (**Fig. 4**). Compared with the wild type, the sizes and numbers of CD68-positive cells were increased in lung, liver, spleen (Fig. 4A), and thymus (data not shown). Frozen sections of liver and lung from 4L/PS-NA mice showed periodic acid-Schiff and CD68 positivities in the same cells (Fig. 4B). This result identifies the storage cells as of macrophage origin. The spleens of 4L/PS-NA mice were significantly ($P = 0.0022$) increased in mass (0.53% of body weight) compared with those from PS-NA mice (0.42%). However, the relative masses of lungs, thymus, and livers were unchanged. The histology of testes and kidneys was normal in all of these mice. Like PS-NA mice (31), 4L/PS-NA and 9H/PS-NA mice had lipid storage cells in the bone marrow from vertebral bodies (data not shown).

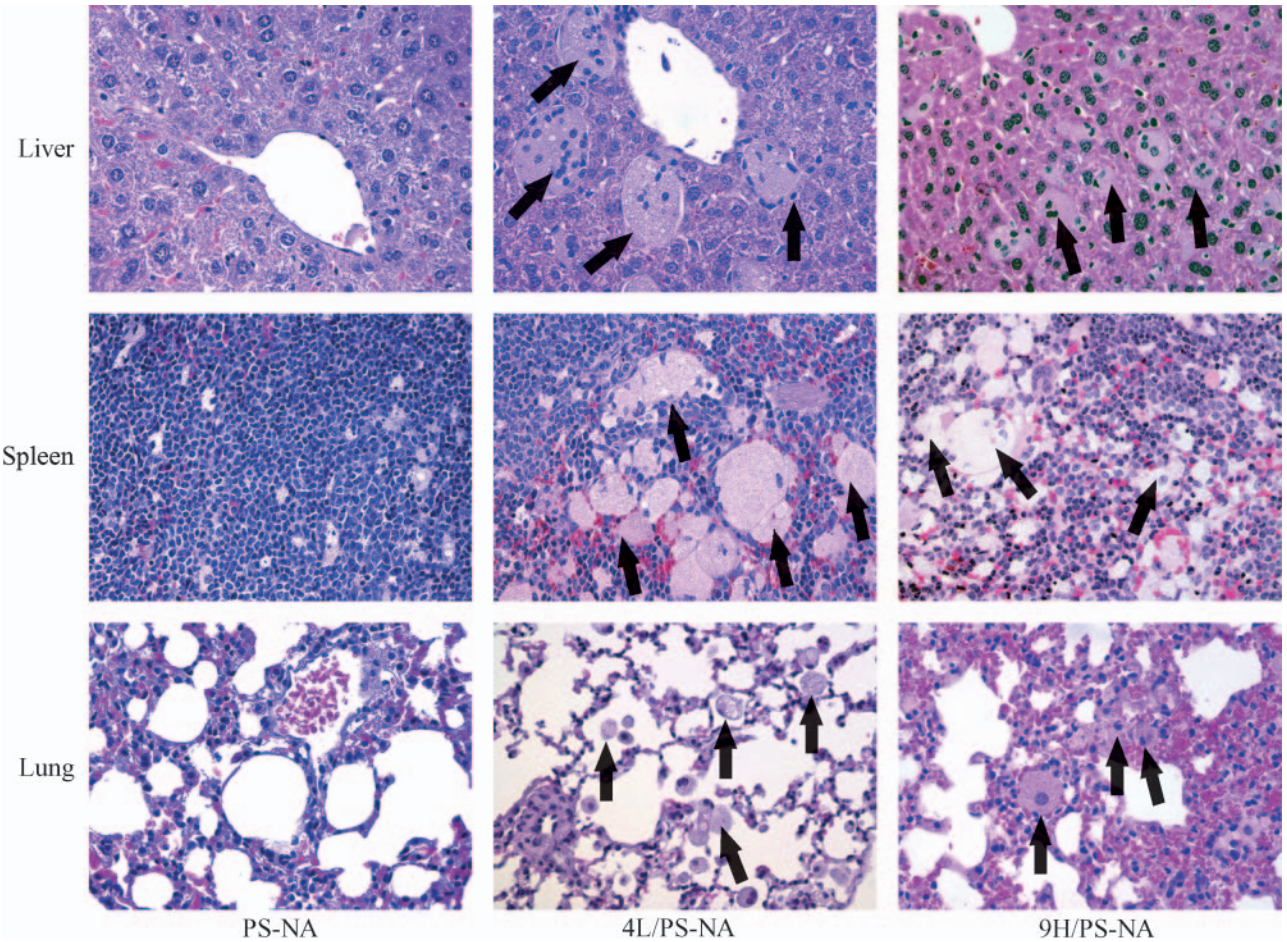

Fig. 2. Storage cells in the visceral tissues of age-matched (22 weeks) PS-NA, 4L/PS-NA, and 9H/PS-NA mice. Hematoxylin and eosin-stained sections of liver, spleen, and lung from PS-NA mice had a normal appearance. In comparison, clusters of lipid storage cells (arrows) were observed in 4L/PS-NA and 9H/PS-NA liver and spleen. Engorged storage cells (arrows) also were present in alveolar and interstitial spaces of the lungs of these mice. Magnifications are 400×.

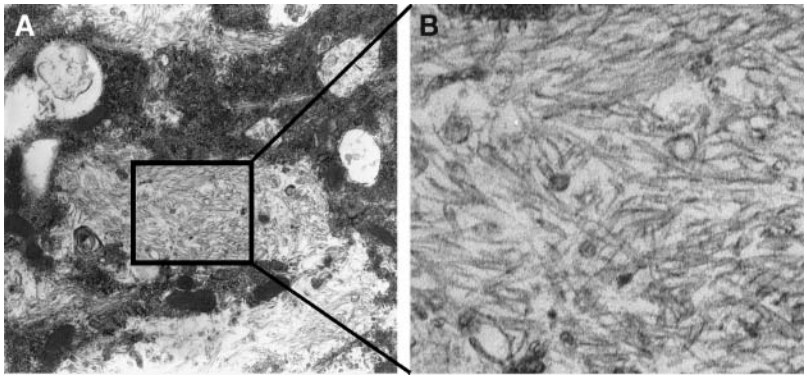

Fig. 3. Electron micrographs of inclusions in 4L/PS-NA mouse lungs. Storage bodies in lung (A; 8,000×) had a characteristic braided structure of glucosylceramide (GC), as observed in Gaucher disease. An enlarged view of the storage bodies is shown in B.

CNS

No gross CNS malformations were found in any of the mice examined in these studies. Throughout their lives (~2 years), V394L/V394L and D409H/D409H did not have any brain pathology, nor did they exhibit neurological abnormalities (8). PS-NA mice developed a neurological phenotype by 3 months (31). The neuropathology of 4L/PS-NA and 9H/PS-NA mice was very similar to that of PS-NA mice (31). The 4L/PS-NA and 9H/PS-NA mice appeared phenotypically normal until ~10 weeks and then developed a slowly progressing CNS phenotype that included gait ataxia, generalized tremor, gross shaking to the point of falling over, and a neurogenic bladder. Lack of rear limb control was the first manifestation. This progressed to almost complete paralysis of the rear limbs by ~20 weeks. The lack of body control eventually resulted in the inability to eat and drink, with consequent malnutrition, dehydration, and demise of these mice (~22 weeks). The neurological phenotype in 4L/PS$^{-/-}$ mice was indistinguishable from that of PS$^{-/-}$ mice (31). Similar to PS-NA mice (31), the neurons of dorsal root ganglia were filled with storage material in 4L/PS-NA and 9H/PS-NA mice. The degenerated neurons in the cerebral cortex and loss of Purkinje cells in the cerebellum were found in such mice >10 weeks old. By electron microcopy, little storage material was seen in Purkinje cells of PS-NA and 4L/PS-NA mice (**Fig. 5A**). Interestingly, the granule cells of 4L/PS-NA mice had large numbers of inclusions at 10 weeks, but very few granule cells contained the inclusions in PS-NA mice at 17.5 weeks (Fig. 5B).

Lipid analyses

The lipid analyses of 4L/PS-NA and 9H/PS-NA mice showed that the major additional lipid accumulated in these mice compared with PS-NA mice was GC (**Fig. 6A**). At 20 weeks, GC was 3- to 10-fold increased in 4L/PS-NA compared with PS-NA mice. GC progressively accumulated from 4 to 20 weeks in livers, spleens, and lungs of 4L/PS-NA mice (Fig. 6B). Small amounts of GC accumulated in age-matched GCase point-mutated (V394L/V394L and D409H/D409H) mouse tissues (8). Predominant lactosylceramide (LacCer) accumulation and slightly increased GC were reported previously in PS-NA and PS$^{-/-}$ mouse tissues (31, 39). In 4L/PS-NA and 9H/PS-NA mice, LacCer was only slightly increased in visceral tissues. These data indicated that the combined deficiency of saposins with GCase point mutations (V394L or D409H) in 4L/PS-NA and 9H/PS-NA mice led to a predominant increase in GC accumulation.

GCase activity and stability

The residual GCase in vitro activity in V394L/V394L mice was ~5–10% of WT levels. PS-NA mice showed reduced GCase activity in visceral tissues by 30–60% (24). Compared with V394L/V394L mice, the GCase activity in 4L/PS-NA mice was decreased significantly in liver ($P = 0.0013$), spleen ($P = 0.0007$), and fibroblasts ($P = 0.0021$) but not in lung and cerebrum (**Fig. 7A**). For 9H/PS-NA, no difference in GCase activity was detectable relative to D409H/D409H mice; this was likely attributable to the variance in measured activity being within the noise level of the error of repeated measures in these assays (data not shown). Strains (C57BL/6J, 129SvEvBrd, or FVB) and mixes of these strains were tested for WT GCase activity. All were found to have equivalent GCase activities (data not shown).

To assess the GCase protein level, fibroblast lysates from WT, PS-NA, 4L/PS-NA, and V394L/V394L mice were analyzed by Western blot analysis using rabbit anti-mouse GCase antibody (Fig. 7B). Relative to WT tissues, the GCase protein level was reduced by ~60% in V394L/V394L fibroblasts and by 90% in 4L/PS-NA fibroblasts. These results imply that the stability of the mutant enzyme was further reduced in the background of a subnormal level of saposins in fibroblasts (24). This lower GCase activity and protein reduced the mutant GCase to a level below which GC accumulated in excess.

DISCUSSION

There have been several attempts to create animal models of Gaucher disease for pathogenic and therapeutic

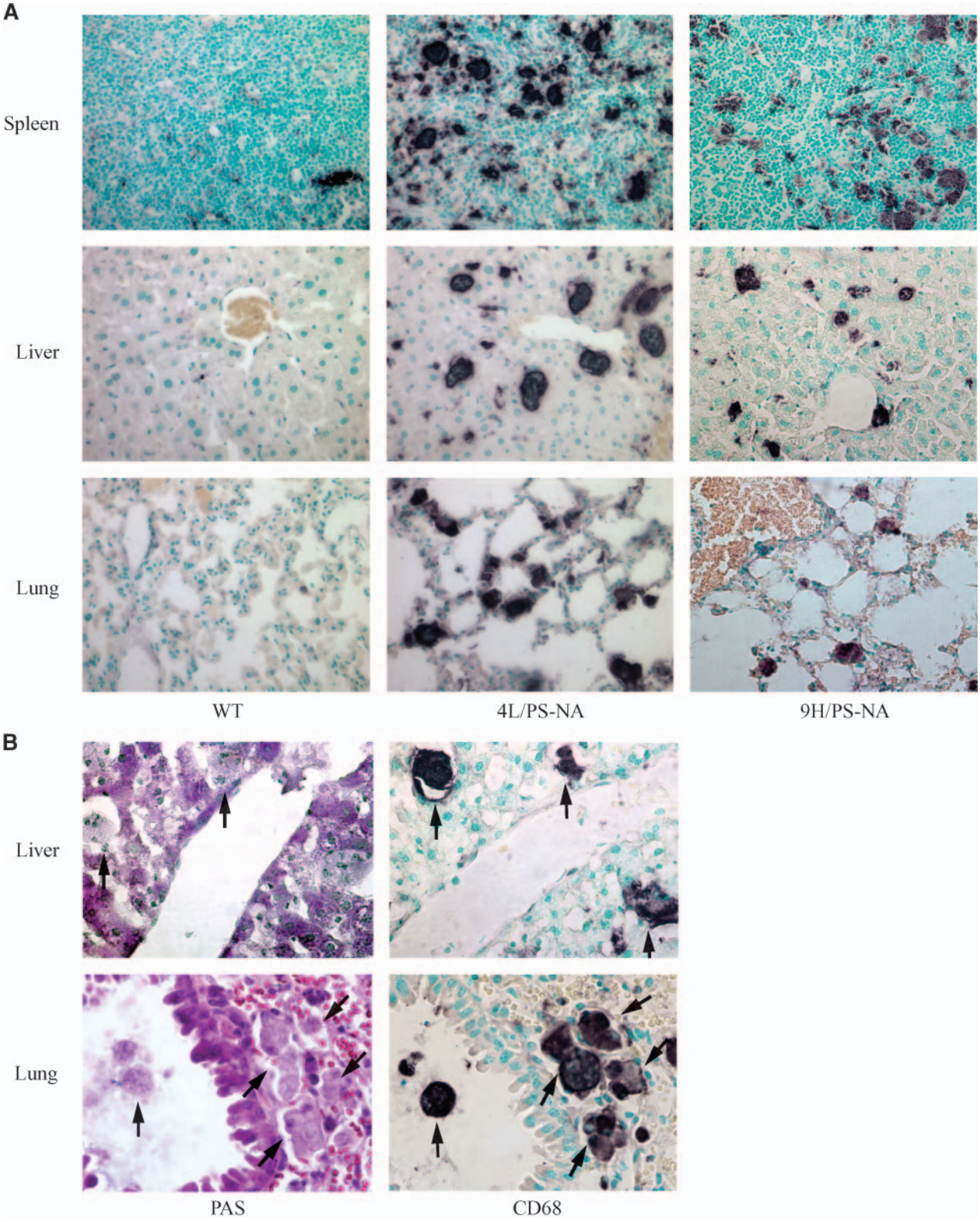

Fig. 4. CD68 staining of cells in the visceral tissues from WT, 4L/PS-NA, and 9H/PS-NA mice. A: Frozen tissue sections from various mice were stained with anti-CD68 (rat anti-mouse) monoclonal antibody (black) and counterstained with methylene green for cell nuclei. Very few CD68-positive cells were in WT spleen, liver, and lung or such tissues from PS-NA mice (not shown). CD68-positive cells were present in large numbers in spleen, liver, and lung of 4L/PS-NA and 9H/PS-NA mice. Magnifications are 400×. B: Frozen tissue sections from 4L/PS-NA mice were stained with periodic acid-Schiff (PAS) and CD68. The periodic acid-Schiff-positive storage cells (arrows) in liver and lung also were CD68-positive, indicating that they were macrophage-derived.

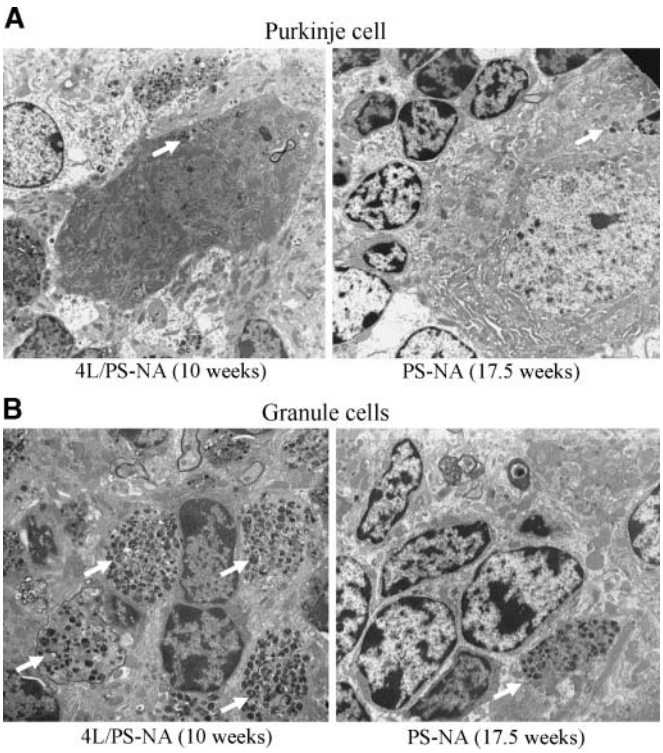

Fig. 5. Electron micrographs of inclusions in cerebellum. A: Purkinje cells in 4L/PS-NA (10 weeks) and PS-NA (17.5 weeks) mice. The inclusions in cells are indicated by arrows. Magnifications are 6,000×. B: Granule cells contained in storage bodies (arrows) in the 4L/PS-NA mouse. Very few cells had storage in the PS-NA mouse (arrow). Magnifications are 7,000×.

studies (6, 7, 42). An ideal model would closely mimic the human disease and rapidly accumulate the substrate GC in Gaucher cells. The null mouse and those created by insertional mutagenesis have been lethal early in life, attributable in part to a skin permeability barrier defect (6, 7). Mice with point mutations at the *gba* locus have exhibited phenotypes ranging from near phenotypic normalcy to biochemical and histological changes similar to the human disease (6–8). Hematopoietic stem cell transplantation of GCase-null cells into WT mice was tested because of the predominant involvement of the macrophage line in human Gaucher disease (42). This resulted in minor abnormalities. Here, a variant of GC storage disease was developed that provides an analog to human Gaucher disease, with characteristic visceral histopathology and biochemical abnormalities. In particular, the homozygous GCase point-mutated mice (V394L, D409H, and D409V) were viable, with low residual activities in all cells but with few storage cells and variable levels of GC accumulation (8). To develop viable, but more severe, models, two genetically modified mice were created based on the known stability effects of saposin C on GCase (24). Because V394L and D409H GCases have abnormal kinetics and stability, we reasoned that partial deficiencies of prosaposin (PS-NA) combined with such point mutations of GCase would further reduce GCase levels in visceral and CNS tissues. We postulated that this GCase level would be below the threshold needed to manifest GC storage. The resultant mice had obvious GC storage primarily in macrophages of visceral organs, and the morphology of the resultant storage cells resembled Gaucher disease cells in the human. However, unlike the human disease, splenic and liver sizes were nearly normal. The CNS clinical course and histopathology resembled those of the PS-NA mice, but with increased accumulation of GC. The 4L/PS-NA and 9H/PS-NA mice were essentially identical, implying that a "floor" of residual activity had been reached, which was consistent with survival without obvious skin abnormalities. Interestingly, attempts to create a D409V/D409V;PS-NA mouse did not result in any live pups with that genotype from >200 pups.

The mechanism by which these mice were created relates primarily to the effects and interactions of saposin C or saposins with the mutant GCases. Theoretically, the lower amounts of saposins produced in the PS-NA mouse would alter WT and mutant enzyme stabilities and activities, as shown in (Fig. 7) and previously demonstrated to be attributable to a proteolytic effect of saposin C (24). Similarly, the residual activity of the various mutant GCases, particularly V394L, was differentially affected and varied closely with the level of prosaposin expressed in various tissues. For example, in liver and spleen, statistically different levels of residual V394L GCase activities were present, and these were in the tissues with the lowest level of expression of saposins. In comparison, lung and brain had 3–10 times higher levels of expression of saposins from the transgene than did liver and spleen. The residual V394L activities in lung and brain were not distinguishable in the 4L/PS-NA or V394L homozygote mice. No difference was found with the D409H mouse homozygotes (because of limited samples) compared with their 9H/PS-NA variants. Obviously, there were detectable differences at a physiological level between the residual activity in each tissue, because GCase in both liver and spleen was decreased significantly compared with the respective levels in lung and brain. Indeed, the progressive GC accumulation in liver, spleen, lung, and cerebellum increased with age and reached levels that were 3–10 times those in the respective age-matched PS-NA mouse tissues. Thus, although a detectable change with the in vitro assay for V394L or D409H activity could not be appreciated, this is evident at a pathophysiological level. Indeed, in fibroblasts from the 4L/PS-NA mice, the GCase protein was decreased substantially compared with that from the V394L homozygotes. This was consistent with the findings in liver and spleen and indicated a stability effect of saposins (especially saposin C) on GCase.

Previously, mouse models based on the point mutations V394L and D409H had been bred into the null mouse background to decrease the level of activity of GCase, at least theoretically, in the respective homozygotes by 50% (i.e., V394L/null and D409H/null would have 50% of the residual activity of the respective homozygotes). Such mice did show progressive accumulations of Gaucher cells and GC in some visceral tissues of advanced age mice (8). The most progressive phenotype developed was based on

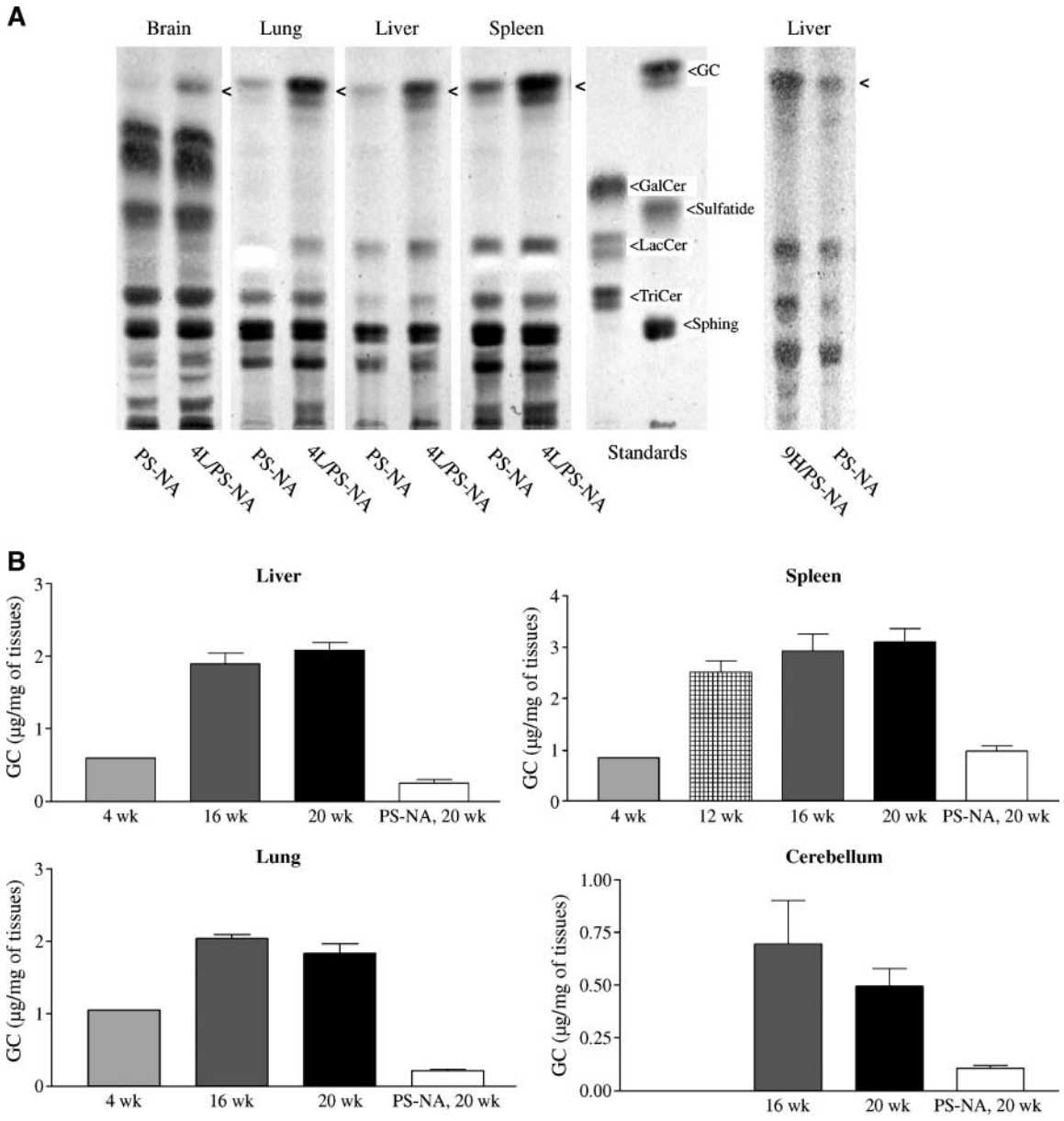

Fig. 6. GC accumulation in 4L/PS-NA and 9H/PS-NA mice. A: Typical TLC of lipid analyses showing increased GC accumulation in 4L/PS-NA tissues compared with PS-NA mice at 12 weeks (left panel). In 9H/PS-NA mice (18 weeks), GC accumulation was increased in liver compared with PS-NA mice at 21 weeks (right panel). Brain refers to a cerebellar hemisphere. The other lipids were unchanged from PS-NA. GalCer, galactosylceramide; LacCer, lactosylceramide; Sphing, sphingomyelin; TriCer, globotriaosylceramide. B: Progressive accumulation of GC with age in 4L/PS-NA tissues compared with PS-NA mice at 20 weeks. Extractions of each tissue from three mice at each age were analyzed. The amount of GC in each tissue was quantitated by densitometric scanning relative to the GC duplicate standards for each mouse.

the D409V/null mouse, which exhibited substantial visceral GC and Gaucher cell accumulation, particularly in spleen and lungs. However, age match comparisons between 4L/PS-NA and 9H/PS-NA mice and V394L/null and D409H/null mice showed much more significant accumulation of Gaucher cells and GC in the present mice with PS-NA. This suggests that the theoretical 50% decrease obtained with a null heteroallele was still above the threshold reached in these current mice to produce significant GC and Gaucher cell accumulation in the various tissues. Of particular interest was the lack of GC accumulation in the brains of the respective heteroallelic homozygotes with the null mice compared with the models developed here, which have substantial additional accumulation of GC compared with PS-NA mice. These results and the fact that we were unable to produce the 9V/PS-NA mice indicate that the models developed here were near a threshold for survivability and manifestations of Gaucher disease in the mouse. An interesting finding in 4L/PS-NA mice was the large number of storage inclusions in granule cells of cerebellum. These are present only very occasionally in PS-NA mice. It is not clear why the granule cells were more vulnerable to GC accumulation. This result supports a cell type-specific threshold for substrate flux.

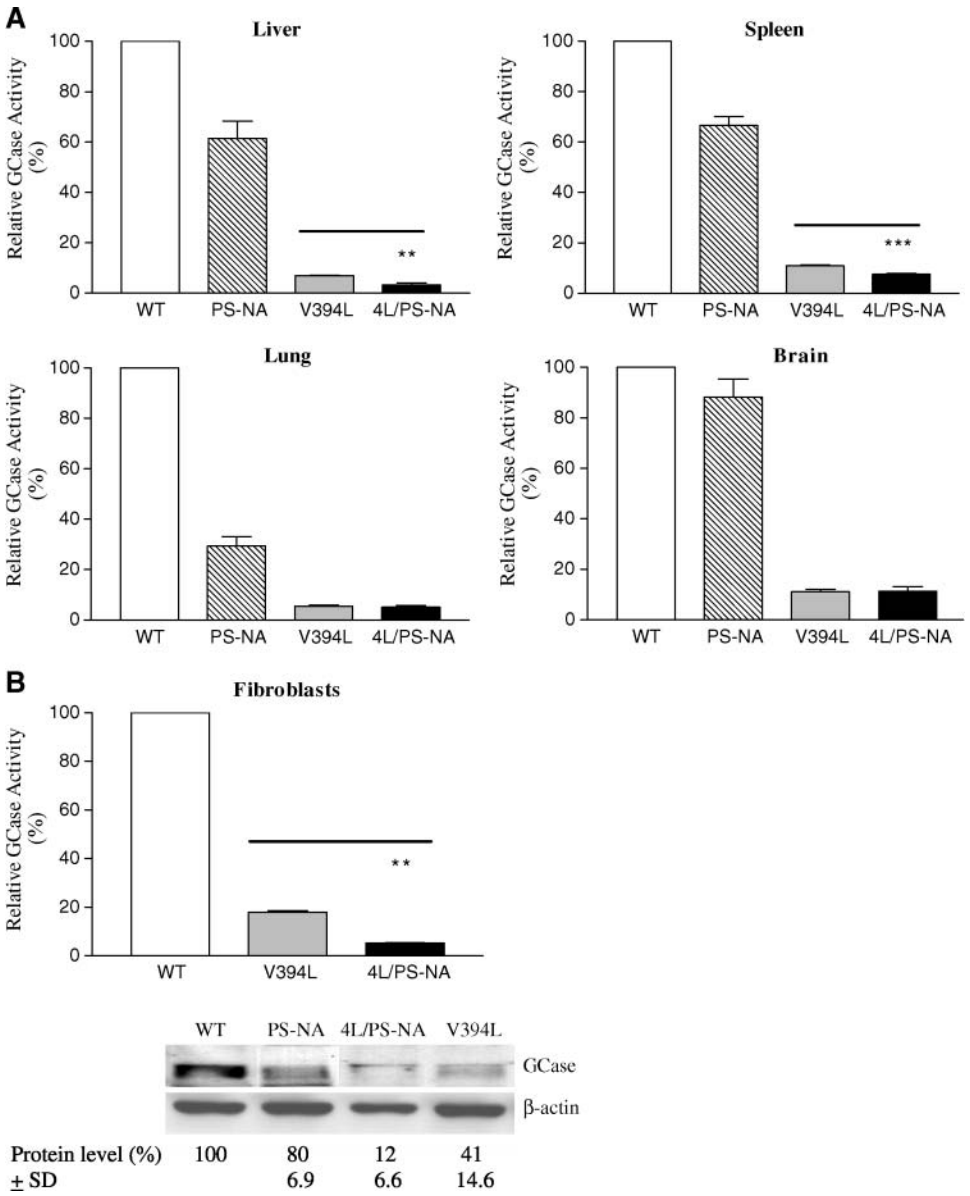

Fig. 7. Acid β-glucosidase (GCase) activity and protein levels in 4L/PS-NA mouse tissues. A: In liver and spleen, GCase activities were decreased significantly in 4L/PS-NA mice compared with V394L/V394L mice. GCase activities in lung and brain were unchanged in 4L/PS-NA and PS-NA mice. ** $P < 0.01$, *** $P < 0.001$ (for comparison of V394L/V394L with 4L/PS-NA tissues; n = 3–5). B: Relative GCase activity and protein levels in cultured fibroblasts. The bar indicates that GCase activities were significantly decreased in 4L/PS-NA cells compared with V394L/V394L. ** $P < 0.01$ (for comparison of V394L/V394L with 4L/PS-NA cells; n = 3). The bottom panel shows that GCase protein ($M_r \sim 60{,}000$) in fibroblasts was detected using rabbit anti-mouse GCase antibody. β-Actin was the loading control. Quantitation was performed with Molecular Dynamics ImageQuant Software using the ratio of GCase/β-actin for normalization. GCase protein levels in PS-NA, 4L/PS-NA, and V394L fibroblasts are presented as percentages of WT levels. Each experiment was repeated in triplicate.

Because of the disruption of glycosphingolipid metabolism in PS-NA mice, one might anticipate an altered flux of glycosphingolipid precursors through the pathways to GC. Indeed, the original intent of the present models was based on the presumption that either the V394L or D409H homozygote would provide a Gaucher disease phenotype in the mouse. The original cross-breeding into PS-NA mice assumed that a decreased flow of substrate (i.e., substrate depletion) through the glycosphingolipid degradative pathway would result in an alleviation of any phenotype. However, the discovery of the proteolytic stabilities and protective effects of saposin C toward GCase negated that presumption. In addition, other than GC, only LacCer was slightly increased. Thus, at least in visceral tissues, the accumulation of GC from hematologic cells appears to proceed unimpeded and leads to no significant abnormalities other than those detected in PS-NA mice initially. Therefore, the mice produced here appear to primarily manifest additional abnormalities related to GCase and not to other parts of the glycosphingolipid pathway.

The progressive accumulation of GC in various tissues, as well as the progressive Gaucher cell infiltrating in these

tissues, provide interesting pathogenetic and, potentially, therapeutic models to evaluate these processes in a mouse model. The development of a variety of therapeutic approaches based on enzyme supplementation, substrate depletion, and gene therapy could be evaluated in such models for effectiveness across the spectrum of involved tissues. However, the models are not homologous, but analogous, to human Gaucher disease, because combined hypomorphism for GCase and prosaposin has not been described in humans. Thus, these models could provide proof of principle, rather than direct transference, for the human Gaucher disease types. These models also provide some insight into the potential interaction of hypomorphic states within a particular pathway leading to exaggerated disease phenotypes.

One might anticipate that therapies based on enzymes, supplementation, or gene therapy might have lesser effects in the PS-NA background because saposin C would be limiting. Preliminary studies with mice containing a tetracycline transactivator-controlled human GCase with liver expression suggest that substantial therapeutic effects of "endogenous enzyme replacement" can be achieved in the background of the PS-NA mouse (unpublished data). In addition, these mouse models could provide an interesting platform to evaluate substrate depletion approaches to Gaucher disease, because GC accumulates substantially in all tissues and, particularly, in the brain. An advantage of these mouse models for substrate depletion evaluation is that CNS and other glycosphingolipids are involved as a result of the PS-NA abnormalities, and the total effect of such approaches could be evaluated in these mice. Finally, one might consider the use of molecular chaperones for the enhancement of endogenous mutant GCase activity in these mice and evaluate the tissue-specific effects. Indeed, we have shown that the V394L mutant enzyme in mouse fibroblasts shows a 4- to 7-fold enhancement of residual enzyme activity when exposed to derivatives of *N*-alkyldeoxynojirimycins at subtoxic levels (unpublished data). This suggests not only a potential for in vivo effects that could be evaluated in the current mouse models but also a potential "mutation-specific effect" that might show greater enhancement relative to some other mutations in the GCase gene.

The authors thank Dr. Keith Stringer for scientific input on the immunohistochemistry study, Humin Ran, Matt Zamzow, Rachel Reboulet, and Andrzej Kazimierczuk for their technical assistance, Lisa McMillin, Meredith Farmer, and Chris Woods for skilled tissue preparation and photomicrographs, and Fannie Anderson for her clerical expertise. This work was supported by grants to G.A.G. from the National Institutes of Health (RO1 NS/DK-36681 and DK-36729).

REFERENCES

1. Beutler, E., and G. A. Grabowski. 2001. Gaucher disease. *In* The Metabolic and Molecular Basis of Inherited Disease, C. R. Scriver, A. L. Beaudet, W. S. Sly, and D. Valle, editors. McGraw-Hill, New York. 3635–3668.
2. Zhao, H., and G. A. Grabowski. 2002. Gaucher disease: perspectives on a prototype lysosomal disease. *Cell. Mol. Life Sci.* **59:** 694–707.
3. Kolodny, E. H., M. D. Ullman, H. J. Mankin, S. S. Raghavan, J. Topol, and J. L. Sullivan. 1982. Phenotypic manifestations of Gaucher disease: clinical features in 48 biochemically verified type 1 patients and comment on type 2 patients. *Prog. Clin. Biol. Res.* **95:** 33–65.
4. Adachi, M., B. J. Wallace, L. Schneck, and B. W. Volk. 1967. Fine structure of central nervous system in early infantile Gaucher's disease. *Arch. Pathol.* **83:** 513–526.
5. Volk, B. W., B. J. Wallace, and M. Adachi. 1967. Infantile Gaucher's disease: electron microscopic and histochemical studies of a cerebral biopsy. *J. Neuropathol. Exp. Neurol.* **26:** 176–177.
6. Tybulewicz, V. L. J., M. L. Tremblay, M. E. LaMarca, R. Willemsen, B. K. Stubblefield, S. Winfield, B. Zablocka, E. Sidransky, B. M. Martin, S. P. Huang, et al. 1992. Animal model of Gaucher's disease from targeted disruption of the mouse glucocerebrosidase gene. *Nature.* **357:** 407–410.
7. Liu, Y., K. Suzuki, J. D. Reed, A. Grinberg, H. Westphal, A. Hoffmann, T. Doring, K. Sandhoff, and R. L. Proia. 1998. Mice with type 2 and 3 Gaucher disease point mutations generated by a single insertion mutagenesis procedure. *Proc. Natl. Acad. Sci. USA.* **95:** 2503–2508.
8. Xu, Y. H., B. Quinn, D. Witte, and G. A. Grabowski. 2003. Viable mouse models of acid β-glucosidase deficiency: the defect in Gaucher disease. *Am. J. Pathol.* **163:** 2093–2101.
9. Tsuji, S., B. M. Martin, J. A. Barranger, B. K. Stubblefield, M. E. LaMarca, and E. I. Ginns. 1988. Genetic heterogeneity in type 1 Gaucher disease: multiple genotypes in Ashkenazic and non-Ashkenazic individuals. *Proc. Natl. Acad. Sci. USA.* **85:** 2349–2352.
10. Charrow, J., H. C. Andersson, P. Kaplan, E. H. Kolodny, P. Mistry, G. Pastores, B. E. Rosenbloom, C. R. Scott, R. S. Wappner, N. J. Weinreb, et al. 2000. The Gaucher registry: demographics and disease characteristics of 1698 patients with Gaucher disease. *Arch. Intern. Med.* **160:** 2835–2843.
11. Theophilus, B., T. Latham, G. A. Grabowski, and F. I. Smith. 1989. Gaucher disease: molecular heterogeneity and phenotype-genotype correlations. *Am. J. Hum. Genet.* **45:** 212–225.
12. Eyal, N., S. Wilder, and M. Horowitz. 1990. Prevalent and rare mutations among Gaucher patients. *Gene.* **96:** 277–283.
13. Pasmanik-Chor, M., S. Laadan, O. Elroy-Stein, A. Zimran, A. Abrahamov, S. Gatt, and M. Horowitz. 1996. The glucocerebrosidase D409H mutation in Gaucher disease. *Biochem. Mol. Med.* **59:** 125–133.
14. Collard, M. W., S. R. Sylvester, J. K. Tsuruta, and M. D. Griswold. 1988. Biosynthesis and molecular cloning of sulfated glycoprotein 1 secreted by rat Sertoli cells: sequence similarity with the 70-kilodalton precursor to sulfatide/GM1 activator. *Biochemistry.* **27:** 4557–4564.
15. Nakano, T., K. Sandhoff, J. Stumper, H. Christomanou, and K. Suzuki. 1989. Structure of full-length cDNA coding for sulfatide activator, a co-β-glucosidase and two other homologous proteins: two alternate forms of the sulfatide activator. *J. Biochem. (Tokyo).* **105:** 152–154.
16. O'Brien, J. S., K. A. Kretz, N. Dewji, D. A. Wenger, F. Esch, and A. L. Fluharty. 1988. Coding of two sphingolipid activator proteins (SAP-1 and SAP-2) by same genetic locus. *Science.* **241:** 1098–1101.
17. Rorman, E. G., V. Scheinker, and G. A. Grabowski. 1992. Structure and evolution of the human prosaposin chromosomal gene. *Genomics.* **13:** 312–318.
18. Furst, W., and K. Sandhoff. 1992. Activator proteins and topology of lysosomal sphingolipid catabolism. *Biochim. Biophys. Acta.* **1126:** 1–16.
19. Grabowski, G. A., S. Gatt, and M. Horowitz. 1990. Acid β-glucosidase: enzymology and molecular biology of Gaucher disease. *Crit. Rev. Biochem. Mol. Biol.* **25:** 385–414.
20. Harzer, K., B. C. Paton, H. Christomanou, M. Chatelut, T. Levade, M. Hiraiwa, and J. S. O'Brien. 1997. Saposins (sap) A and C activate the degradation of galactosylceramide in living cells. *FEBS Lett.* **417:** 270–274.
21. Kishimoto, Y., M. Hiraiwa, and J. S. O'Brien. 1992. Saposins: structure, function, distribution, and molecular genetics. *J. Lipid Res.* **33:** 1255–1267.
22. Qi, X., and G. A. Grabowski. 2001. Molecular and cell biology of acid β-glucosidase and prosaposin. *Prog. Nucleic Acid Res. Mol. Biol.* **66:** 203–239.
23. Sandhoff, K., T. Kolter, and G. Van Echten-Deckert. 1998. Sphingolipid metabolism. Sphingoid analogs, sphingolipid activator pro-

teins, and the pathology of the cell. *Ann. N. Y. Acad. Sci.* **845:** 139–151.
24. Sun, Y., X. Qi, and G. A. Grabowski. 2003. Saposin C is required for normal resistance of acid β-glucosidase to proteolytic degradation. *J. Biol. Chem.* **278:** 31918–31923.
25. Schnabel, D., M. Schroder, and K. Sandhoff. 1991. Mutation in the sphingolipid activator protein 2 in a patient with a variant of Gaucher disease. *FEBS Lett.* **284:** 57–59.
26. Leonova, T., X. Qi, A. Bencosme, E. Ponce, Y. Sun, and G. A. Grabowski. 1996. Proteolytic processing patterns of prosaposin in insect and mammalian cells. *J. Biol. Chem.* **271:** 17312–17320.
27. Vielhaber, G., R. Hurwitz, and K. Sandhoff. 1996. Biosynthesis, processing, and targeting of sphingolipid activator protein (SAP) precursor in cultured human fibroblasts. Mannose 6-phosphate receptor-independent endocytosis of SAP precursor. *J. Biol. Chem.* **271:** 32438–32446.
28. Kondoh, K., T. Hineno, A. Sano, and Y. Kakimoto. 1991. Isolation and characterization of prosaposin from human milk. *Biochem. Biophys. Res. Commun.* **181:** 286–292.
29. Sun, Y., D. P. Witte, and G. A. Grabowski. 1994. Developmental and tissue-specific expression of prosaposin mRNA in murine tissues. *Am. J. Pathol.* **145:** 1390–1398.
30. Cohen, T., W. Auerbach, L. Ravid, J. Bodennec, A. Fein, A. H. Futerman, A. L. Joyner, and M. Horowitz. 2005. The exon 8-containing prosaposin gene splice variant is dispensable for mouse development, lysosomal function, and secretion. *Mol. Cell. Biol.* **25:** 2431–2440.
31. Sun, Y., X. Qi, D. P. Witte, E. Ponce, K. Kondoh, B. Quinn, and G. A. Grabowski. 2002. Prosaposin: threshold rescue and analysis of the "neuritogenic" region in transgenic mice. *Mol. Genet. Metab.* **76:** 271–286.
32. Wells, M. A., and J. C. Dittmer. 1963. The use of Sephadex for the removal of nonlipid contaminants from lipid extracts. *Biochemistry.* **172:** 1259–1263.
33. Dreyfus, H., B. Guerold, L. Freysz, and D. Hicks. 1997. Successive isolation and separation of the major lipid fractions including gangliosides from single biological samples. *Anal. Biochem.* **249:** 67–78.
34. Igisu, H., H. Takahashi, and K. Suzuki. 1983. Abnormal accumulation of galactosylceramide in the kidney of twitcher mouse. *Biochem. Biophys. Res. Commun.* **110:** 940–944.
35. Xu, Y. H., E. Ponce, Y. Sun, T. Leonova, K. Bove, D. Witte, and G. A. Grabowski. 1996. Turnover and distribution of intravenously administered mannose-terminated human acid β-glucosidase in murine and human tissues. *Pediatr. Res.* **39:** 313–322.
36. Grace, M. E., K. M. Newman, V. Scheinker, A. Berg-Fussman, and G. A. Grabowski. 1994. Analysis of human acid β-glucosidase by site-directed mutagenesis and heterologous expression. *J. Biol. Chem.* **269:** 2283–2291.
37. Qi, X., T. Leonova, and G. A. Grabowski. 1994. Functional human saposins expressed in *Escherichia coli*. Evidence for binding and activation properties of saposins C with acid β-glucosidase. *J. Biol. Chem.* **269:** 16746–16753.
38. Qi, X., K. Kondoh, H. Yin, M. Wang, E. Ponce, Y. Sun, and G. A. Grabowski. 2002. Ex vivo localization of the mouse saposin C activation region for acid β-glucosidase. *Mol. Genet. Metab.* **76:** 189–200.
39. Fujita, N., K. Suzuki, M. T. Vanier, B. Popko, N. Maeda, A. Klein, M. Henseler, K. Sandhoff, and H. Nakayasu. 1996. Targeted disruption of the mouse sphingolipid activator protein gene: a complex phenotype, including severe leukodystrophy and wide-spread storage of multiple sphingolipids. *Hum. Mol. Genet.* **5:** 711–725.
40. Madar-Shapiro, L., M. Pasmanik-Chor, A. M. Vaccaro, T. Dinur, A. Dagan, S. Gatt, and M. Horowitz. 1999. Importance of splicing for prosaposin sorting. *Biochem. J.* **337:** 433–443.
41. Lee, R. E. 1968. The fine structure of the cerebroside occurring in Gaucher's disease. *Proc. Natl. Acad. Sci. USA.* **61:** 484–489.
42. Beutler, E., C. West, B. E. Torbett, and H. Deguchi. 2002. A chimeric mouse model of Gaucher disease. *Mol. Med.* **8:** 247–250.